Supplementary Material

Supplementary Methods

MRI imaging

Functional and anatomical images were acquired on a 3 Tesla Skyra whole-body MRI scan (Siemens, Erlangen, Germany). Anatomical images were collected using a T1-weighted MP-RAGE sequence (1 mm isotropic, TE= 2,2 ms, TR=2200 ms, TI=900 ms, flip angle=8°), and a FLAIR sequence (1 mm isotropic, TE 349 ms, TR 6600 ms, TI 2300 ms). Functional images consisted in a series of 180 BOLD images (TR=2 s, TE=30 ms, flip angle 90°, 2.5 mm isotropic) acquired while the patient was at rest with his eyes closed, both on- and off-treatment.

The analysis of resting-state data was performed using Statistical Parametric Mapping (SPM12) (http://www.fil.ion.ucl.ac.uk/spm), with the functional connectivity (CONN) toolbox (http://web.mit.edu/swg/software.htm), both written in the MATLAB language (http://www.mathworks.com). Images were preprocessed using all CONN default parameters, including realignment, co-registration with structural images, normalization, band-pass filtering (0.008 Hz–0.09 Hz), smoothing (8mm Gaussian). White matter and cerebrospinal fluid signals were treated as regressors of non-interest. The temporal correlation between voxels was used to derive, both on- and off-treatment, (1) maps of Global Correlation, which consists, for each voxel, in the average of its correlation with all other voxels; (2) maps of seed-to-voxel correlation, which consists, for each voxel, in the value of its correlation with the average signal in a given region of interest (ROI). Specifically, we used the left and right intra-calcarine ROIs from the atlas provided with the CONN toolbox. Maps of R values were Fisher-transformed; the maps from the on- and off-treatment states were then subtracted and divided by the standard deviation of the difference, resulting in maps of Z scores. Those were thresholded at $p<0.001$ ($Z>3.09$) voxelwise, plus a cluster-size threshold of 100 voxels. Surface rendering of resting state results in Figure 2 were created with the bspmview toolbox (http://www.bobspunt.com/bspmview).

Positron emission tomography (PET)

18Fluorodeoxyglucose (FDG) PET scans were acquired both on- and off-treatment following the same procedure: acquisition was performed with a hybrid PET/CT system (Biograph mCT Flow - Siemens Healthcare) 30 min after the i.v. injection of FDG (2 MBq/Kg) and lasted 10 min. The patient rested in quiet surroundings with his eyes closed at least 20 min before and 30 min after the injection. Images were reconstructed using iterative reconstruction and corrected for gamma-ray attenuation and scatter.

PET volumes were co-registered, spatially normalized in the Montreal Neurological Institute (MNI) space using SPM, smoothed using an isotropic Gaussian kernel of 8 mm, and normalized in intensity with proportional scaling to conduct voxel-by-voxel comparisons with a normal database of FDG images (29 healthy volunteers, age 46.0±13.5 y/o, range [20-69], 16 men). Two-sample T-tests were used to compare the patient's metabolism to normal controls, to identify cortical or subcortical regions of reduced glucose metabolism in off- and on-treatment conditions. A threshold of $p<0.05$ corrected for multiple comparisons with the family-wise-error (FWE) method was applied. Only clusters of more than 100 voxels (0.8 cc) were considered. Analyses were restricted within a cortical mask of the bilateral occipital cortex as defined with the AAL atlas.

Supplementary Figure 1

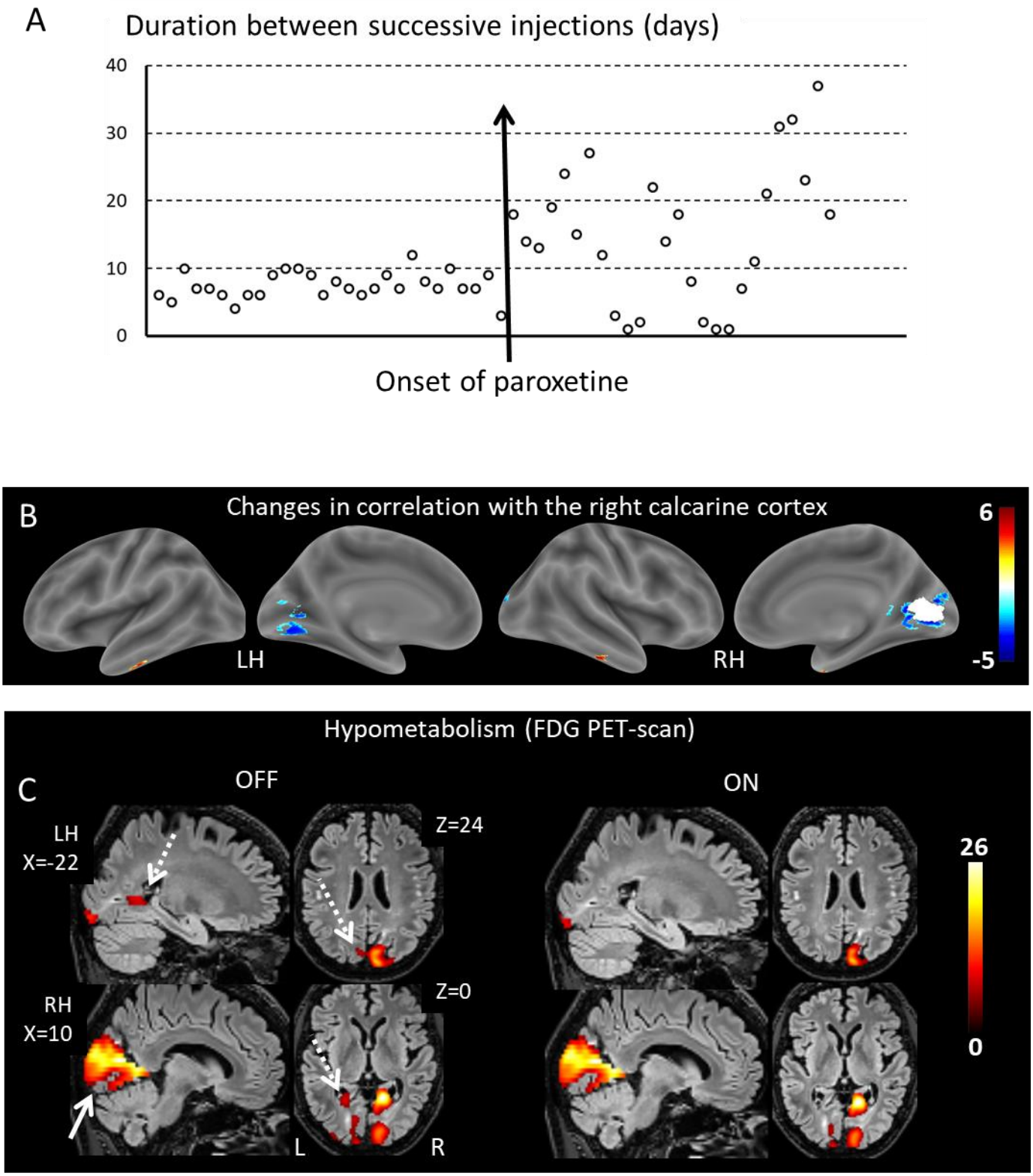

Legend for Supplementary Figure 1:

(A) Duration of the effect of mepivacaïne, as indexed by the lag between successive injections over a period of 2 years. The addition of paroxetine yielded a doubling of the average duration, with an increase in variability.

(B) With mepivacaine, there were no substantial changes in the pattern of distant correlation of the lesioned right calcarine region (white).

(C) As compared to control subjects, PET-scan showed hypometabolism in the areas affected on anatomical MRI. In the off-mepivacaine state, hypometabolism had an overall larger volume, and extended to apparently intact regions in the left (dotted arrows) and right (solid arrow) occipital cortex.

Color scales represent Z scores.

Supplementary Figure 2

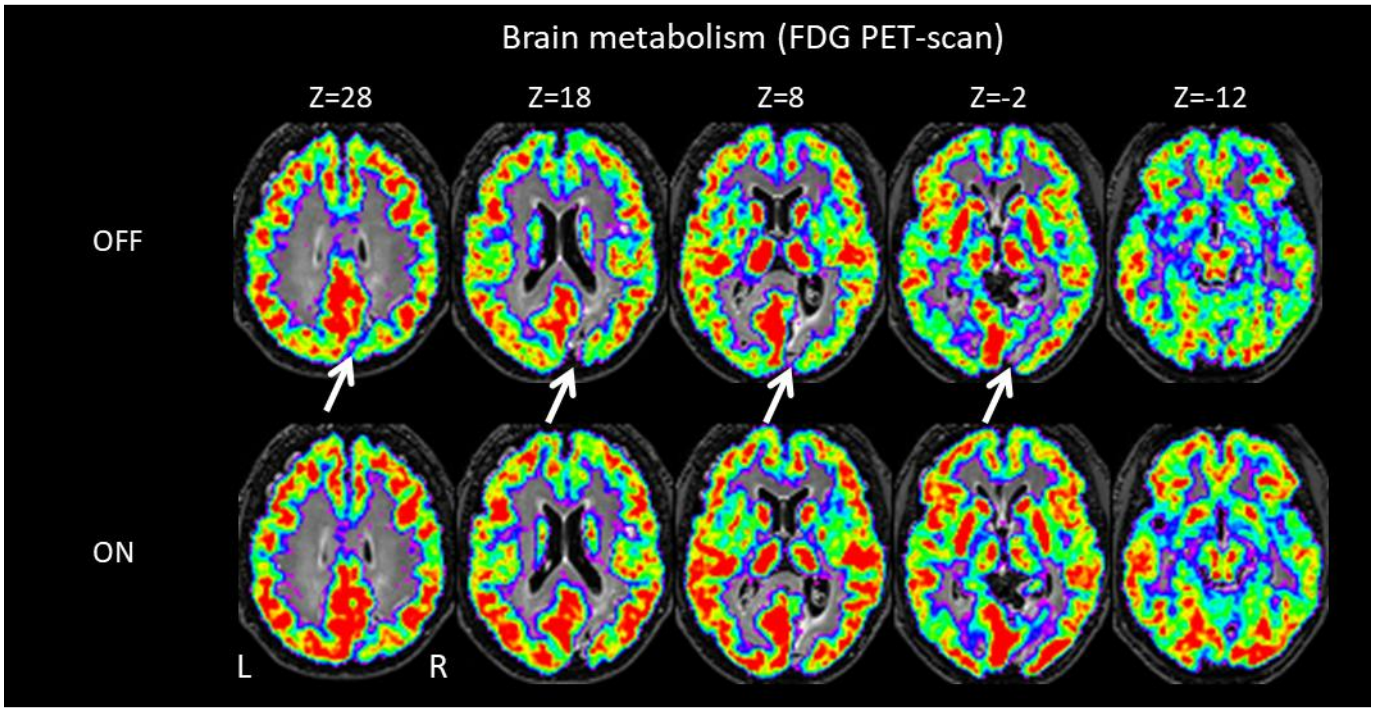

Legend for Supplementary Figure 2:

The patient's brain metabolism as assessed with PET-scan, showing hypometabolism mostly visible in the right occipital lobe (white arrow).

Supplementary Table 1

Birmingham object recognition battery	
Copying	9/9
Length Match Task	26/30 (z=0,56)
Size Match Task	28/30 (z=0,29)
Orientation Match Task	25/30 (z=0,08)
Position of Gap Match Task	37/40 (z=0,48)
Minimal Feature View Test	25/25 (z=0,85)
Foreshortened View Task	25/25 (z=1,31)
Drawing from Memory	6/6
Object Decision Task	26/32 (z=0,45)
Function Match Task	31/32 (z=0,45)
Associative Match Task	29/30 (z=0,63)
Other tests	
Benton's Judgment of Line Orientation	14/15
Hooper Visual Organization Test	27/30 (z=1,30)
OD 80 picture naming test	80/80
Facial recognition test	**38/54**
Block design test (WAIS-IV)	53/66
Matrix reasoning test (WAIS-IV)	22/26
Mini Mental State, Frontal Assessment Battery, Trail Making Test, Wisconsin Cards Sorting Test, Stroop Test, Five Words Test, California Verbal Learning Test, digit and visuospatial span	Normal

When right hemianopia was suppressed with mepivacaine, the patient still had left hemianopia but showed normal performance on tests assessing high-level visuoperception, visuoconstruction, visuospatial reasoning, and general cognitive abilities. He scored just below the normal level only on Benton's facial recognition test (bold).

Supplementary Table 2

PET-scan hypometabolism in the patient as compared to 29 healthy controls								
P corr	**kE**	***P FWE-corr***	***T***	**MNI Coordinates**			**Location**	**Brodman area**
cluster-level		**voxel-level**		**x**	**y**	**z**		
OFF mepivacaine, whole brain								
0.000	3951	0.000	38.7	16	-60	9	R. calcarine	17
0.000	648	0.000	14.7	-12	-94	-7	L. lingual	18
0.000	594	0.000	17.7	12	9	-13	R. olfactory	25
0.000	617	0.000	10.3	0	38	28	L. frontal sup medial	9
0.000	522	0.000	10.0	0	55	12	R. frontal sup medial	10
0.000	115	0.000	10.4	7	-9	12	R. thalamus	
0.000	527	0.000	30.7	43	-74	-39	R. cerebellum	
0.000	361	0.000	10.2	4	-53	-46	R. cerebellum	
ON mepivacaine, whole brain								
0.000	3664	0.000	37.6	16	-60	9	R. calcarine	17
0.000	499	0.000	13.9	-12	-94	-7	L. lingual	18
0.000	532	0.000	15.2	7	9	-13	L. frontal sup medial	25
0.000	444	0.000	10.9	3	34	29	R. frontal sup medial	8
0.000	301	0.000	11.0	7	-11	10	R. thalamus	
0.000	801	0.000	32.8	43	-73	-40	R. cerebellum	
0.000	614	0.000	10.8	-4	-53	-46	L. cerebellum	
OFF mepivacaine, occipital mask								
0.000	3888	0.000	35.3	16	-57	2	R. lingual	19
0.000	124	0.000	8.9	-17	-58	5	L. lingual	18
ON mepivacaine, occipital mask								
0.000	2509	0.000	34.7	16	-57	2	R. lingual	19
0.000	626	0.000	13.3	-12	-93	-7	L. lingual	18

References of tests used for the neurovisual assessment

1. Riddoch MJ, Humphreys GW. Birmingham Object Recognition Battery (BORB). Philadelphia: Psychology Press; 1993.

2. Benton A, Sivan A, Hamsher K, Varney N, Spreen O. Contributions to Neuropsychological Assessment. New York: : Oxford University Press; 1994.

3. Deloche G, Hannequin D. Test de dénomination orale d'images DO80. Paris: Les Editions du Centre de Psychologie Appliquée; 1997.

4. Wechsler D. Echelle d'Intelligence de Wechsler pour Adultes - 4e édition (WAIS-IV): Les éditions du Centre de Psychologie Appliquée; 2011.

5. Hooper HE. The Hooper visual organization test. Los Angeles: Western Psychological Services; 1983.